

1 **Complete Glutaraldehyde elimination during Chitosan hydrogel drying by SC-**
2 **CO₂ processing**

3 Lucia Baldino, Simona Concilio *, Stefano Cardea *, Iolanda De Marco, Ernesto Reverchon

4 Department of Industrial Engineering, University of Salerno,

5 Via Giovanni Paolo II, 132, 84084, Fisciano (SA), Italy

6

7

8

9 Authors information:

10 Lucia Baldino lbaldino@unisa.it; Ph: 0039-089-964232

11 Iolanda De Marco idemarco@unisa.it; Ph: 0039-089-964066

12 Ernesto Reverchon ereverchon@unisa.it; Ph: 0039-089-964116

13

14 *Corresponding authors:

15 Simona Concilio sconcilio@unisa.it; Ph: 0039-089-964115

16 Stefano Cardea scardea@unisa.it; Ph: 0039-089-969365

1 **Abstract**

2 Chitosan (CH) is one of the polymers most frequently proposed in form of hydrogels for
3 tissue engineering (TE) applications. It is often crosslinked with the aim of improving its stability
4 and mechanical properties. In this work, for the first time, a supercritical carbon dioxide (SC-CO₂)
5 gel drying process was proposed to obtain CH scaffolds and simultaneously eliminate unreacted
6 glutaraldehyde (GTA), taking advantage of its solubility in supercritical mixtures.

7 SC-CO₂ gel dried crosslinked CH aerogels showed a nanofibrous structure characterized by
8 an average diameter of about 100 nm. No collapse of the nanostructure was observed in the
9 aerogels, due to the peculiarities of supercritical fluids (near zero surface tension). Moreover,
10 crosslinked CH showed a thermally stable structure, as determined by TGA analysis. The
11 hypothesis that a supercritical mixture is able to efficiently extract GTA residues entrapped in the
12 gel matrix was also verified: negligible residues of GTA were found at the end of release
13 experiments; in particular, at the best operating conditions, a GTA concentration equal to 0.013
14 ppm was detected. Therefore, the produced crosslinked CH aerogels can be effectively and safely
15 used for TE applications.

16

17 **Keywords:** Glutaraldehyde, Chitosan, Supercritical CO₂, Aerogel, Scaffold.

18

1 **1 Introduction**

2 Tissue damage or organ failure are among the most frequent and devastating problems in
3 medicine. Current therapeutic approaches (allografts, xenografts, autografts and implantation of
4 biomedical devices) have largely improved the quality of life; but they are associated with some
5 limitations including donor availability, infection transmission, poor integration and potential
6 rejection of the implant. Tissue engineering (TE) has the aim to overcome such limitations finding
7 new therapies for the treatment of tissue diseases, with the basic idea to repair or re-create tissues or
8 organs, restoring impaired functions (Barry, Gidda, Scotchford & Howdle, 2004; Eichhorn &
9 Sampson, 2005).

10 Several TE strategies depend on the preparation of polymeric scaffolds, that can operate as a
11 synthetic extra cellular matrix (ECM) to organize cells into a three-dimensional architecture and to
12 stimulate formation and growth of a desired tissue (Yang, Leong, Du & Chua, 2001). Depending on
13 the tissue of interest and on the specific application, the required scaffold material and its properties
14 can be quite different; but, for all tissues, it is required (Ma, 2004): 1) a 3-D structure similar to the
15 tissue to be substituted; 2) a very high porosity with an open-pore geometry and suitable pore size;
16 3) nanostructural characteristics mimicking ECM; 4) mechanical properties suitable to maintain the
17 predesigned tissue structure and to support the specific loadings applied to the original tissue; 5)
18 biocompatibility and a proper degradation rate; 6) absence/reduced toxic and inflammatory
19 response.

20 Various techniques have been reported in the literature for the fabrication of biodegradable
21 scaffolds, such as gas foaming, fiber bonding, solvent casting/particulate leaching, phase separation,
22 freeze drying, electrospinning and 3D-printing; but, these techniques suffer several limitations. In
23 particular, it is very difficult to simultaneously obtain the macro, micro and nanostructural
24 characteristics that have previously been described (Reverchon & Cardea, 2012).

25 Among the polymeric materials proposed for TE applications, water-soluble polymers have
26 been frequently used in form of hydrogels (Park & Lakes, 2007). They are formed by hydrophilic

1 polymer chains and can be either of synthetic or of natural origin. The structural resistance of
2 hydrogels depends on crosslinks formed between polymer chains via chemical bonds and/or
3 physical interactions. Physically bonded hydrogels used in TE applications have structural
4 properties similar to the ECM, can be processed under moderately mild conditions, , and can be
5 used in a minimally invasive manner (Lee & Mooney, 2001). However, it is difficult to accurately
6 control gel pore size, chemical functionalization, dissolution and degradation; moreover,
7 mechanical properties are limited. Consequently, these hydrogels often provide inconsistent in vivo
8 performances (Dash, Chiellini, Ottenbrite & Chiellini, 2011). A way to improve hydrogel properties
9 is the creation of irreversible networks formed by chemical bonds. In these cases, polymer chains
10 are covalently bonded together by small cross-linker molecules, secondary polymerization, or
11 irradiation.

12 Hydrogels can also be used or stored in dried form; the most used technique to obtain these
13 structures is freeze-drying. This technique is suitable for a wide range of hydrogel materials,
14 including natural (Jin, Moreira Teixeira, Dijkstra, Karperien, Zhong & Feijen, 2008; Lv, Hu, Feng
15 & Cui, 2008) and synthetic hydrophilic polymers (Lee, Kang, Kim & Son, 2008; Lin, Yu & Yang,
16 2006). However, hydrogels architecture is extremely sensitive to the quenching process and can
17 totally or partially collapse due to the interfacial tension of the liquid during solvent evaporation
18 (Ho et al., 2004). Another limitation of the freeze-drying process is due to the frequent formation of
19 a surface skin and to the partial collapse of the structure at the scaffold-air interface; in addition,
20 freeze-drying is energy intensive and requires relatively long processing times for the solvent
21 removal (Quirk, France, Shakesheff & Howdle, 2004).

22 Chitosan (CH) is obtained by deacetylation of the natural biopolymer chitin. Both chitosan
23 and chitin are chemically similar to cellulose, differing only by the functional group situated at
24 Carbon-2 of the monomeric unit. The presence of free amine groups in chitosan enhances the
25 solubility and reactivity of this polymer with respect to chitin and cellulose. Some products
26 obtained by chemical modification of chitosan found applications in various fields (Dash, Chiellini,

1 Ottenbrite & Chiellini, 2011; Dutta, Dutta & Tripathi, 2004; Harish Prashanth & Tharanathan,
2 2007; Ravi Kumar, 2000). For example, covalent chitosan cross-linked hydrogels are obtained by
3 attacking photo-reactive or enzyme-sensitive molecules on the polymer, followed by their exposure
4 to UV or sensitive enzymes. The properties of cross-linked hydrogels mainly depend on their cross-
5 linking density and by the ratio between cross-link molecules and polymer repeating units (Park,
6 Park & Shalaby, 2011).

7 Chitosan hydrogels are frequently crosslinked using glutaraldehyde (GTA) that is one of the
8 most effective crosslinking agents; the interest in modifying chitosan using GTA has recently
9 increased in many potential applications, especially in biomedical and environmental field (Alves &
10 Mano, 2008; Berger, Reist, Mayer, Felt, Peppas & Gurny, 2004; Dash, Chiellini, Ottenbrite &
11 Chiellini, 2011; Krajewska, Zaborska & Leszko, 1997; Kurita, Yoshino, Nishimura, Ishii, Mori &
12 Nishiyama, 1997; Ma et al., 2003; Payne, Chaubal & Barbari, 1996). The limitations due to the use
13 of GTA (frequently used as a powerful sterilizing agent) are related to its high cytotoxicity (Zeiger,
14 Gollapudi & Spencer, 2005). This characteristic is known by a long time; Speer et al. found that
15 even a 3.0 ppm GTA concentration inhibited fibroblast growth in tissue culture at 99% (Speer,
16 Chvapil, Eskelson & Ulreich, 1980). Therefore, it is desirable to efficiently eliminate GTA after
17 crosslinking (Choy, Cheng, Choi & Kim, 2008); unfortunately, this operation is usually not
18 performed, and/or its success is limited by mass transfer resistance encountered by liquid solvents
19 in solid media.

20 Supercritical carbon dioxide (SC-CO₂) has been successfully used in several improved
21 processes to produce micro and nanoparticles (Adami, Liparoti & Reverchon, 2011; De Marco,
22 Knauer, Cice, Braeuer & Reverchon, 2012; Du, Shen, Tang, Guan, Yao & Zhu, 2014; Liparoti,
23 Adami & Reverchon, 2012; Marra, De Marco & Reverchon, 2012; Montes, Gordillo, Pereyra, De
24 los Santos & Martínez de la Ossa, 2014) and porous materials (Baldino, Cardea, De Marco &
25 Reverchon, 2014; Baldino, Cardea & Reverchon, 2014; Cardea, Baldino, Pisanti & Reverchon,
26 2014; Cardea, Baldino, Scognamiglio & Reverchon, 2014; Cardea & Reverchon, 2011; Duarte,

1 Mano & Reis, 2009; Karimi, Heuchel, Weigel, Schossig, Hofmann & Lendlein, 2012). Recently, a
2 SC-CO₂ based gel drying process has also been proposed to produce 3-D scaffolds (Pisanti, Yeatts,
3 Cardea, Fisher & Reverchon, 2012; Reverchon, Cardea & Rapuano, 2008), preserving macro and
4 nanostructure of the gel. Indeed, efficient solvent elimination and short processing times can be
5 obtained due to the large affinity of SC-CO₂ with almost all the organic solvents. In this specific
6 process, SC-CO₂ forms a supercritical mixture with the organic solvent used to produce the gel, that
7 is, then, eliminated maintaining zero surface tension inside its solid structure. This operation avoids
8 gel collapse. However, SC-CO₂ shows a very limited affinity with water at the ordinary
9 temperatures and pressures used in SC-CO₂ processing; for example, at 40 °C and 100 bar, water
10 solubility is around 0.5 % w/w (Sabirzyanov, Il'in, Akhunov & Gumerov, 2002). Therefore, the
11 described process is not directly applicable to polymeric hydrogels, and some water-ethanol
12 exchange steps have to be performed to substitute with ethanol the water contained in the gel before
13 SC-drying (Della Porta, Del Gaudio, De Cicco, Aquino & Reverchon, 2013; García-González,
14 Alnaief & Smirnova, 2011).

15 In this work, we propose, for the first time, SC-CO₂ gel drying of CH scaffolds with the
16 simultaneous elimination of unreacted GTA, taking advantage of GTA solubility in supercritical
17 mixtures. Operating in this manner, we can obtain improved CH scaffolds for TE applications that
18 maintain the original nanofibrous structure of the gel, and do not contain residues of the highly
19 cytotoxic crosslinking agent that, if not removed, does not allow the proliferation of cells in the
20 scaffold. CH-GTA aerogels will be characterized from a macroscopic and microscopic point of
21 view and a study of the release of GTA residues will be performed.

22

23 **2 Materials, apparatuses and methods**

24 Chitosan with Low M_w (Deacetylation 75 – 85 %, viscosity 20 - 300 cps) and Medium M_w
25 (Deacetylation 75 – 85 %, viscosity 200 - 800 cps) were purchased from Sigma-Aldrich (St. Louis,
26 MO); Acetic Acid glacial (99.9 % purity) and Sodium Hydroxide (NaOH) were bought from Carlo

1 Erba Reagenti (Rodano, Mi - Italy); Carbon Dioxide (99 % purity) was bought from SON (Società
2 Ossigeno Napoli - Italy). Glutaraldehyde solution 25 % w/w in water was purchased from Sigma-
3 Aldrich. Distilled water was produced using a laboratory water distiller supplied by ISECO S.P.A.
4 (St. Marcel, Ao - Italy). All materials were used as received.

5

6 **2.1 Preparation of Chitosan aerogel**

7 Two kinds of CH (Low M_w and Medium M_w) were used, starting from two different CH
8 concentrations (2 and 5 % w/w) in acid water (water to acetic acid ratio 95:5). The best preparation
9 of CH hydrogel was the following: Chitosan Medium M_w (0.40 g) was dissolved in 20 mL of
10 water/acetic acid solution (pH 2.43) to obtain a CH concentration of 2 % w/w. NaOH (1 M in water,
11 pH 14) was slowly added to this solution and the changes in pH were registered, each added mL, by
12 a pH-meter. At the same time, the gel formation was monitored, until the attainment of the
13 maximum gel point that was reached at pH 12.5. Then, the gel sample was repeatedly washed with
14 distilled water to remove the excess of NaOH solution.

15 CH hydrogels were crosslinked using a GTA solution 0.25 % w/w in water. The
16 crosslinking solution was obtained by diluting 1 mL of GTA (25 % w/w) in 99 mL of water.
17 Different ratios CH gel/GTA were used (see Table 1), to identify the best operating conditions:
18 CH:GTA 32:1, 16:1, 8:1, 4:1 and 1:1; GTA content was increased to the maximum ratio (1:1) to
19 verify the efficacy of the SC-CO₂ purification process on crosslinked CH aerogel.

20

CH:GTA	32:1	16:1	8:1	4:1	1:1
CH hydrogel, mL	10	3	3	3	3
GTA 0.25 % w/w, mL	0.3	0.2	0.4	0.75	3

21 **Table 1.** CH and GTA amounts used for the crosslinking reaction.

22

1 The crosslinking reaction was performed at room temperature, adding GTA solution to CH
2 gel, under Vortex shaking for 1 min. The system was left for three days in quiet. Then, the
3 crosslinked sample was repeatedly washed with distilled water. SC-CO₂ drying cannot be directly
4 applied in the case of hydrogels, since SC-CO₂ shows a very reduced affinity with water (Diamond
5 & Akinfiev, 2003). Therefore, before drying, the samples were immersed in an ethanol bath for 24 h
6 at room temperature, to allow the complete replacement of water with ethanol inside the samples.

7

8 **2.2 SC-CO₂ gel drying description**

9 Samples were prepared in a homemade laboratory plant that mainly consists of a 316
10 stainless steel cylindrical high-pressure vessel with an internal volume of 80 mL, equipped with a
11 high pressure pump (mod. LDB1, Lewa, Germany) used to deliver SC-CO₂. Pressure in the vessel
12 was measured by a test gauge (mod. MP1, OMET, Italy) and regulated using a micrometering valve
13 (mod. 1335G4Y, Hoke, SC, USA). Temperature along the plant was regulated using PID
14 controllers (mod. 305, Watlow, Italy). At the exit of the vessel, a rotameter (mod. D6, ASA, Italy)
15 was used to measure CO₂ flow rate.

16 SC-CO₂ gel drying was performed according to the following procedure: the vessel was
17 closed and filled from the bottom with SC-CO₂. When the required pressure and temperature were
18 obtained (200 bar and 35 °C), drying was performed with a SC-CO₂ flow rate of about 1 kg/h, that
19 corresponds to a residence time inside the vessel of about 4 min; drying lasted 8 h. A
20 depressurization time of 20 min was used to bring back the system at atmospheric pressure.

21

22 **2.3 Analytical methods**

23 To perform Field Emission Scanning Electron Microscopy (FESEM), the samples were
24 cryo-fractured using liquid Nitrogen; then, they were sputter coated with Gold (Agar Auto Sputter
25 Coater mod. 108 A, Stansted, UK) at 30 mA for 160 s and analyzed using a FESEM (mod. LEO

1 1525, Carl Zeiss SMT AG, Oberkochen, Germany) to evidence the micro and nanostructure and to
2 measure the diameter of the fibers forming the structure.

3 A Perkin Elmer Lambda 900 Spectrophotometer (Milano, Italy) was used, working in time-
4 drive mode at a fixed wavelength of 234 nm (maximum absorption for GTA) for the study of GTA
5 release from the CH aerogels. The concentration of GTA released in the Phosphate Buffer Solution
6 (PBS) was detected by UV-absorption spectra recorded as a function of time. In a typical
7 experiment, 15 mL of CH hydrogel were immersed in 3 mL of PBS buffer (pH 7.4) and glycine 0.1
8 M (PBS:Gly = 0.43). Glycine role is to suppress the pH decrease normally observed in sodium
9 phosphate buffer salt, possibly by reducing the nucleation rate of salt and thereby decreasing the
10 extent of buffer salt crystallization. GTA absorbance was measured at 234 nm, using a UV-Vis
11 spectrophotometer at room temperature (Bigi, Cojazzi, Panzavolta, Rubini & Roveri, 2001).

12 FT-IR spectra were recorded using a Thermo Nicolet Nexus Spectrometer (Rodano (MI),
13 Italy), equipped with Attenuated Total Reflection (ATR) sampling, working with a Zinc selenide
14 crystal.

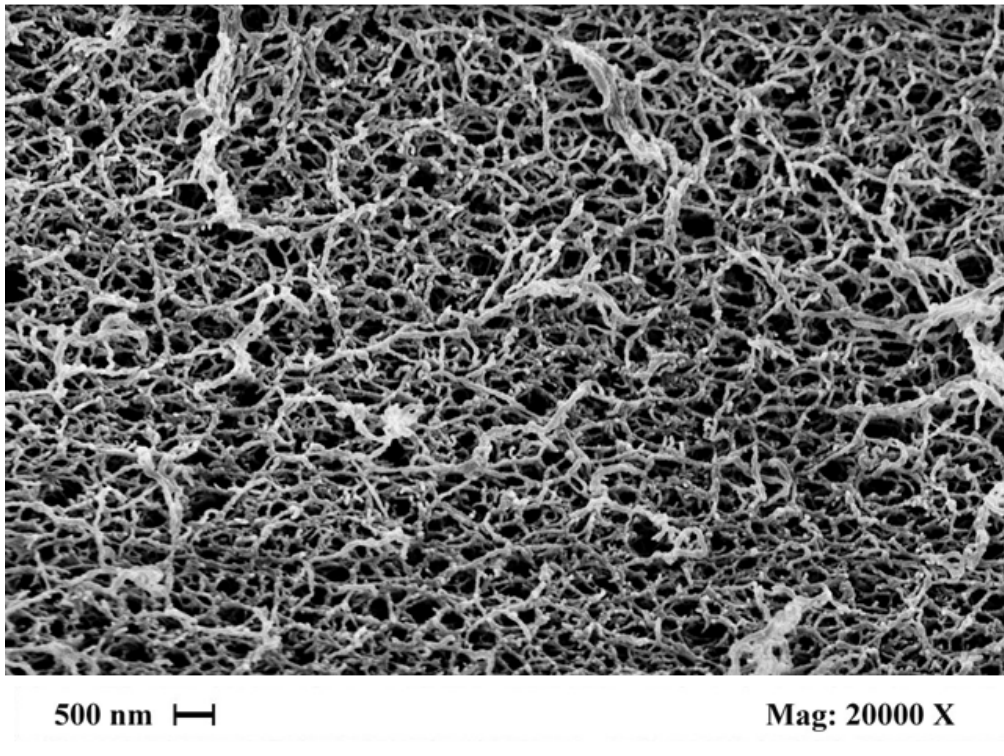
15 The thermal behavior of CH aerogels was examined by thermogravimetric analysis (TGA)
16 (Q600, TA Instruments, Milano, Italy), online connected to a quadrupole mass detector (Quadstar
17 422, Pfeiffer Vacuum, USA) in Nitrogen atmosphere at a scanning rate of 10 K/min.

18

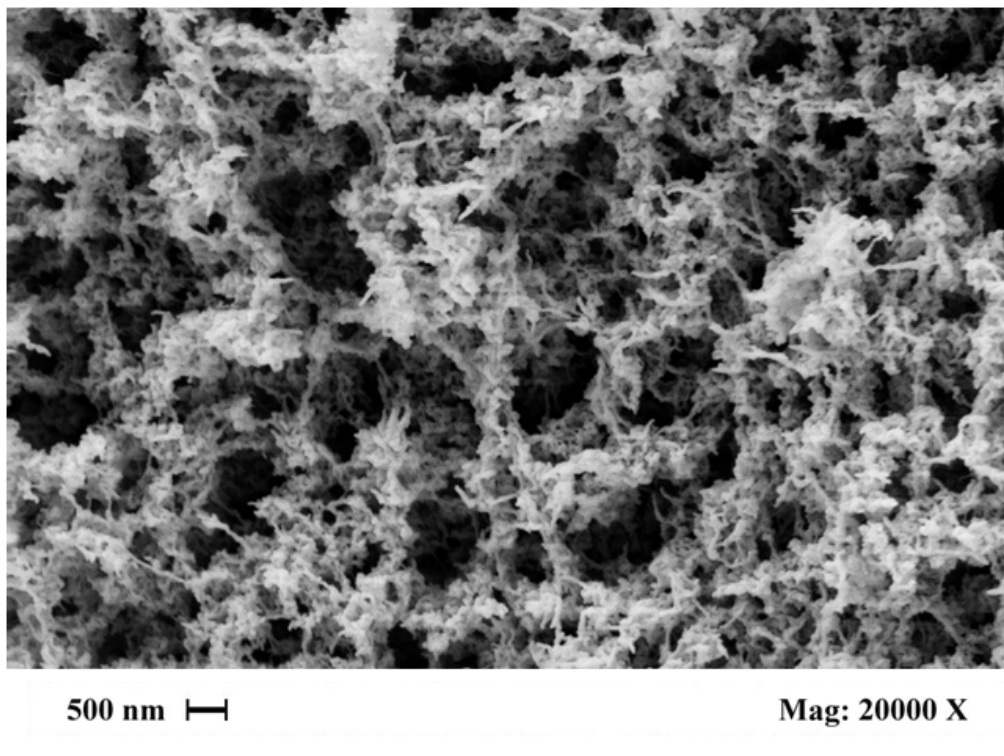
19 **3 Results and Discussion**

20 In the first part of the study, some experiments were performed to optimize the CH hydrogel
21 in water. We found that, at the end of the drying process, the samples maintained the same shape
22 and volume, which is the first evidence that the delicate nanofibrous architecture of CH gels was
23 not destroyed. This evidence was confirmed by the FESEM images, taken at the same enlargement,
24 reported in Figure 1a-d, in which both CH aerogel (Figure 1a) and crosslinked CH aerogel (Figure
25 1b-d) showed the same nanofibrous morphology. The nanofibers are very regular and uniformly
26 distributed along the samples section and have an average size of about 100 nm. The only

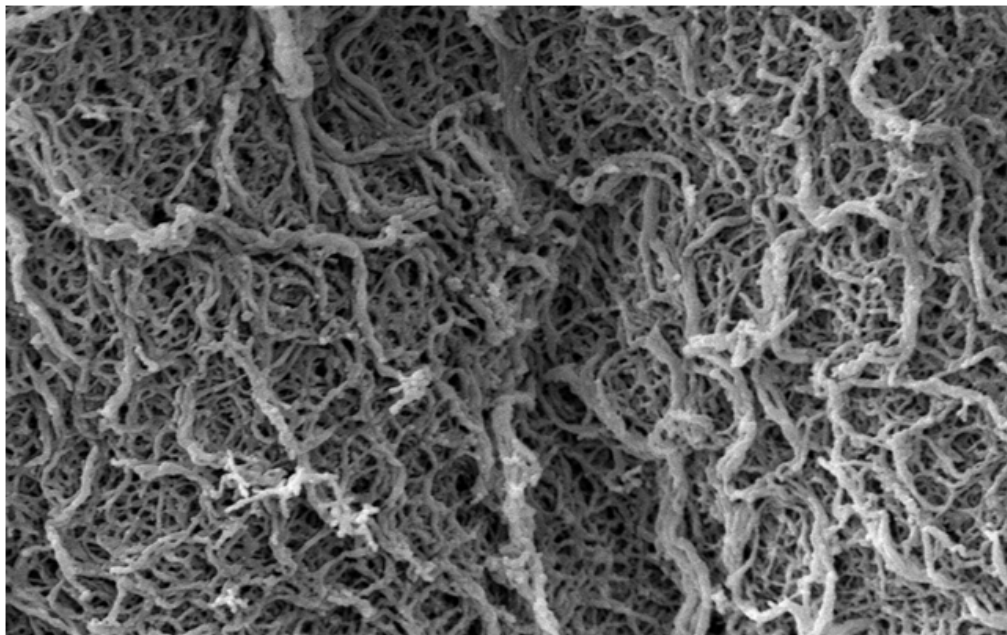
- 1 difference between Figure 1 images is related to the different arrangement of the nanofibers that
2 could depend on the quantity of GTA used for crosslinking.



(a)



(b)



500 nm

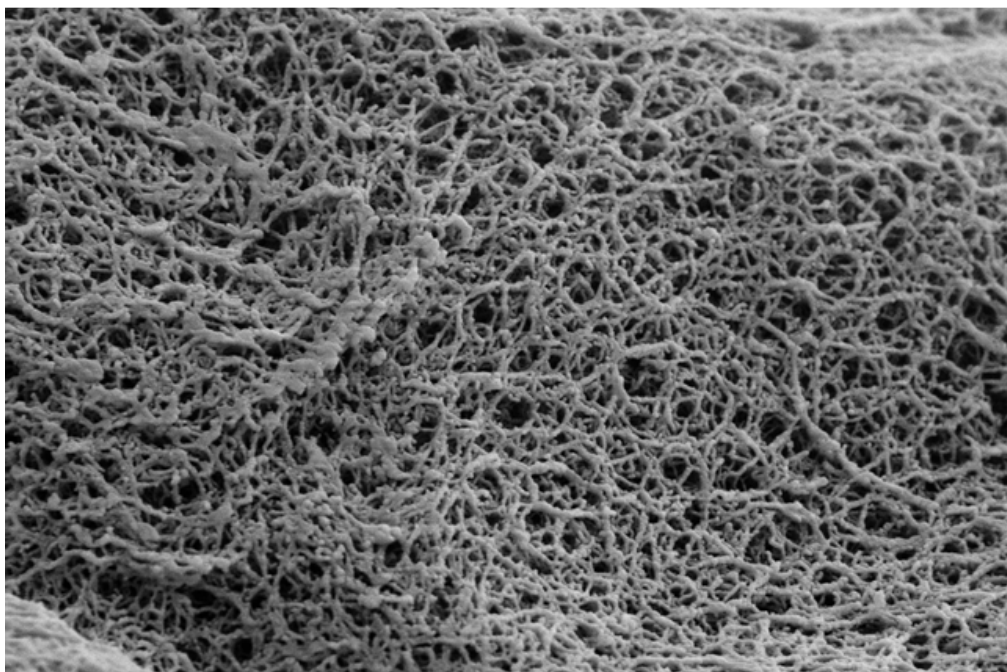
Mag: 20000 X



1

(c)

2



500 nm

Mag: 20000 X



3

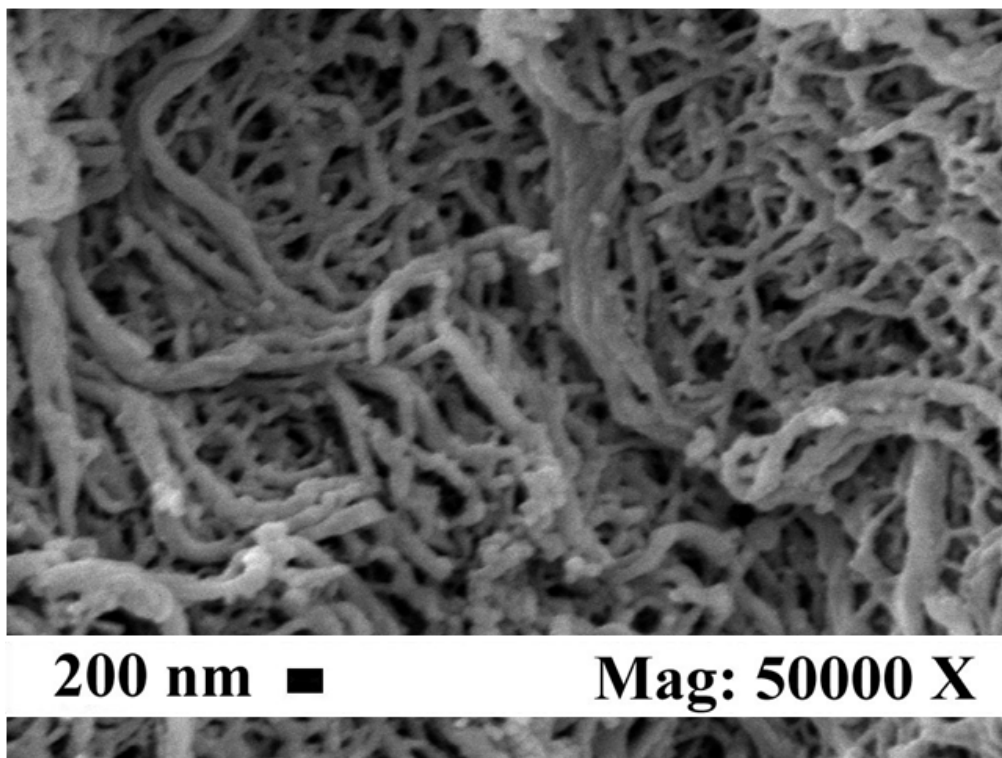
(d)

4

5 **Figure 1.** FESEM images of Chitosan medium M_w (2 % w/w): (a) CH aerogel section; (b) CH:GTA
6 16:1 aerogel section; (c) CH:GTA 8:1 aerogel section; (d) CH:GTA 4:1 aerogel section.

1 Also the samples surface maintained the uniform and nanofibrous morphology, as shown,
2 for example, in Figure 2, where a FESEM image of the surface of a CH:GTA 4:1 aerogel is
3 reported. On the contrary, as discussed in the Introduction, aerogels produced by freeze-drying
4 show closed surfaces, due to the force exerted by the surface tension during the solvent extraction
5 from the polymeric matrix, which causes the polymer collapse.

6



7

8 **Figure 2.** FESEM image of CH:GTA 4:1 aerogel surface.

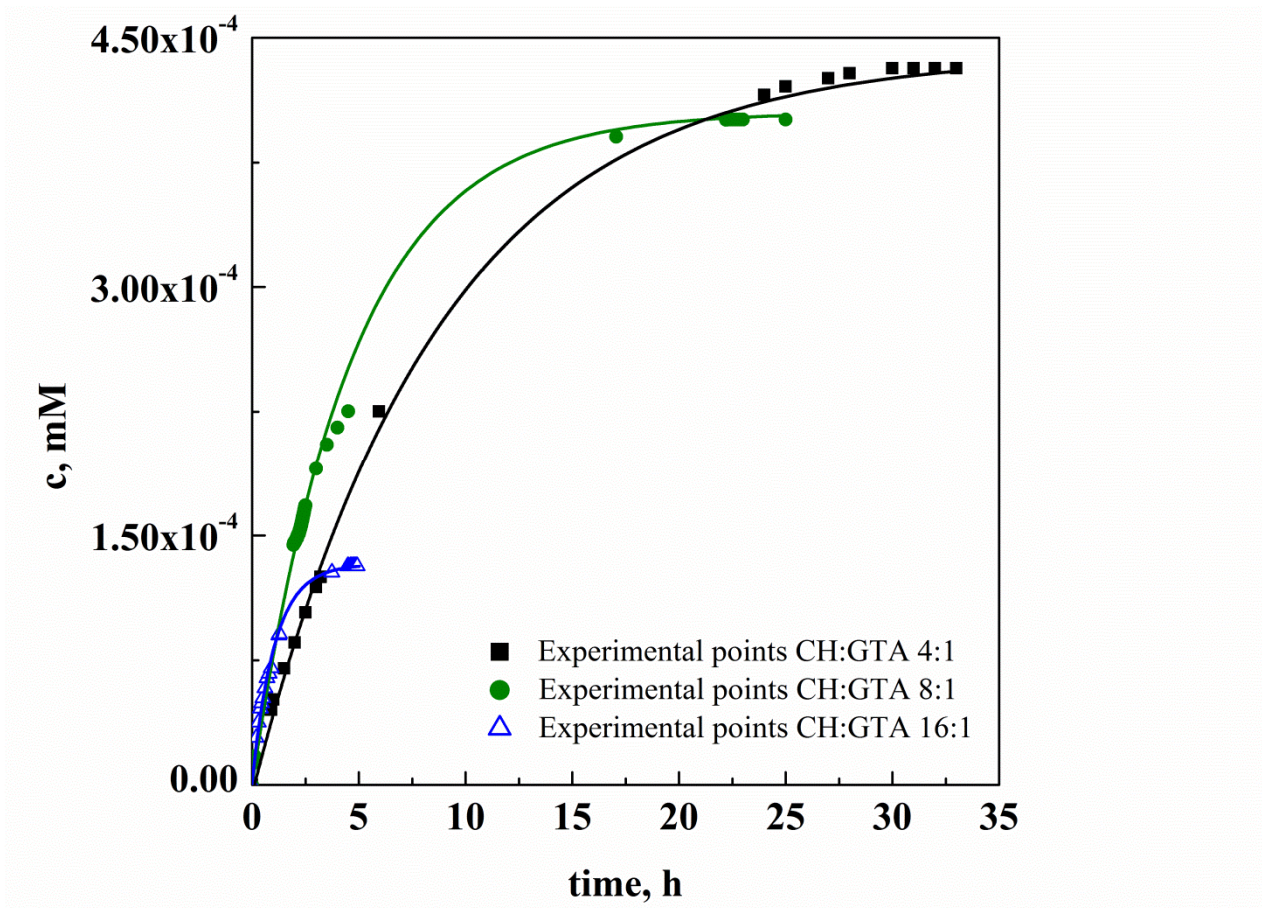
9

10 This result is important to favor the interaction of cells with the aerogel, since open skins are
11 required for the cell inoculation, adhesion and proliferation; it means that this morphology improves
12 the efficiency of the cells culture. Summarizing, nanostructured gel morphology was preserved in
13 all the cases and it is similar to that of the ECM proteins of the native tissues, that show an average
14 fibers diameter between 50-500 nm; i.e., 1 to 2 orders of magnitude smaller than the living cells.
15 This characteristic allows the cells to be in direct contact with many ECM fibers, thereby defining
16 their three dimensional orientation (Barnes, Sell, Boland, Simpson & Bowlin, 2007).

1

2 **3.1 Glutaraldehyde release from Chitosan aerogel**

3 The second problem in CH hydrogel drying is the entrapment inside the structure of
4 unreacted GTA. It can be reduced by washing several times the samples with ethanol to extract at
5 least part of the GTA and using calibrated quantities of GTA to induce crosslinking, reducing at a
6 minimum the unreacted material. However, since GTA (as shown in the Introduction) is a powerful
7 sterilizing agent, the possibility of extracting its residues during the drying process can generate a
8 great improvement of the final product characteristics, in view of its application for cells
9 cultivation. Indeed, being GTA a small molecule, its solubility in SC-CO₂ (not known at the best of
10 our knowledge) could be low. Moreover, during SC-drying, CO₂ extracts ethanol contained in the
11 alcogel, forming a SC-mixture ethanol-CO₂. This mixture shows more affinity with GTA than SC-
12 CO₂ alone, due to the presence of ethanol in which GTA is largely soluble. In addition, gas-like
13 diffusivity of the supercritical ethanol-CO₂ mixture can allow a more efficient GTA extraction with
14 respect to the one attainable using liquid ethanol. To verify experimentally this hypothesis, a series
15 of GTA release experiments was performed. GTA concentration was measured using a calibration
16 curve obtained using known quantities of GTA; the released GTA curves and the final
17 concentration values (in terms of ppm) are respectively reported in Figure 3 and Table 2.



1
2
3

Figure 3. GTA release from CH aerogels at 2 % w/w.

Aerogel	GTA concentration, ppm
CH:GTA 1:1	77.7
CH:GTA 4:1	$4.32 \cdot 10^{-2}$
CH:GTA 8:1	$4.01 \cdot 10^{-2}$
CH:GTA 16:1	$1.32 \cdot 10^{-2}$

4
5

Table 2. Maximum GTA concentration measured in the release medium.

6 The sample CH:GTA 1:1, in which the quantity of GTA used for crosslinking is in a large
7 excess, was not reported in Figure 3. In all the other cases, the obtained asymptotic curves were
8 fitted using an exponential equation. The GTA released from the samples is maximum (about 0.04
9 ppm) for the CH:GTA ratios equal to 4:1 and 8:1 and is about 0.01 ppm for CH:GTA ratio equal to

1 16:1. These amounts are, for all the samples, negligible if compared to the value of 3 ppm reported
2 in literature as the GTA residue that blocks, almost completely, cells reproduction (Speer, Chvapil,
3 Eskelson & Ulreich, 1980). These values clearly indicate that these materials can be readily used for
4 tissue engineering applications.

5

6 **3.2 FTIR analysis**

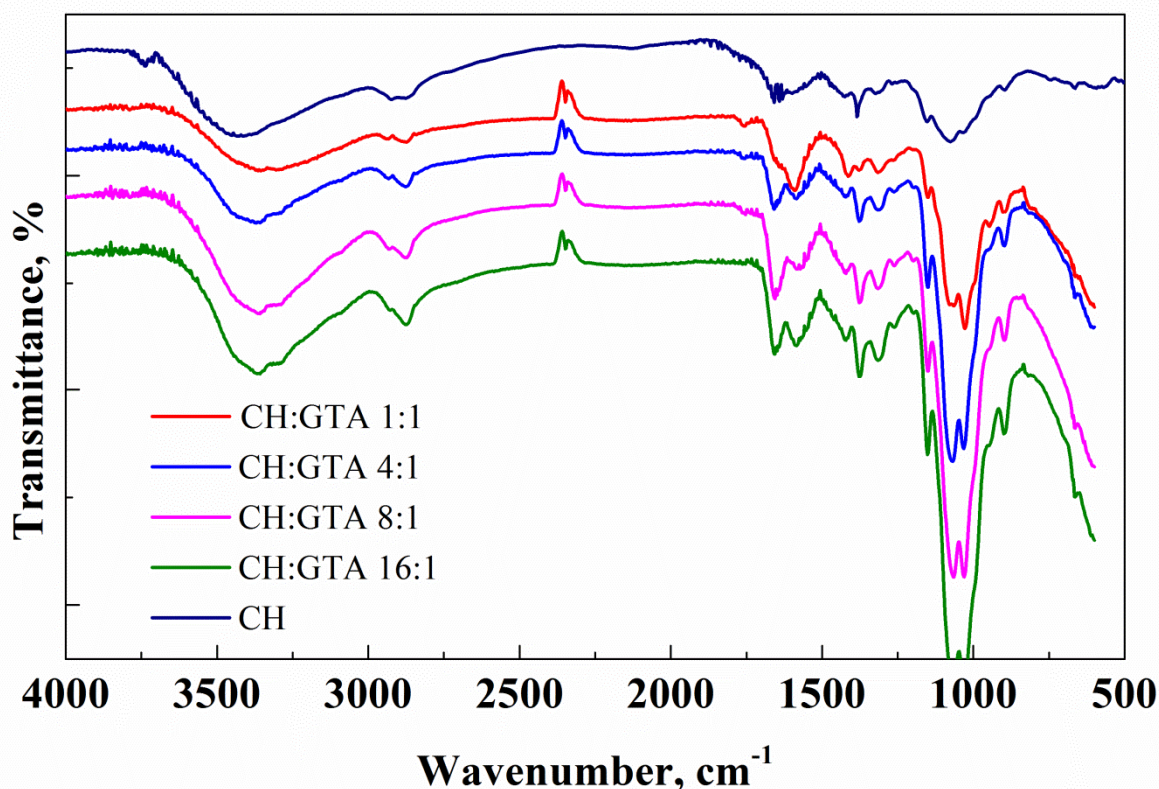
7 IR spectroscopy was used to evaluate the structural modifications induced by the
8 crosslinking of chitosan with GTA. In Figure 4, FTIR spectra obtained with ATR method on
9 samples of CH 2 % w/w are shown. In particular, the following sample curves are reported: pure
10 CH (used as a reference), CH:GTA 16:1, 8:1, 4:1 and 1:1. The last sample (1:1) contained a large
11 GTA excess and was used only to verify the efficiency of the SC-CO₂ based purification process on
12 crosslinked aerogels.

13 FTIR spectrum of pure CH (Figure 4, first curve from the top) shows the typical band at
14 3360 cm⁻¹ of OH and NH₂ stretching. The peak at 2874 cm⁻¹ belongs to stretching vibration of CH
15 groups. In all the spectra, two peaks are visible at 1650 cm⁻¹ and 1640 cm⁻¹, which can be attributed
16 to C=O stretching and NH bending of amide groups (note that CH we used had a deacetylation
17 degree of 80 %). The peak at 1376 cm⁻¹ can be assigned to methyl groups of the polymer and the
18 one at 1420 cm⁻¹ to the bending of O-H and C-H groups.

19 For all the samples (from 16:1 to 1:1 ratios), a peak at 1590 cm⁻¹, belonging to the imine
20 C=N bond, formed between the amine residues of CH and the aldehyde terminals of the GTA, is
21 well detectable. At the same time, it can be noticed that only in the CH:GTA 1:1 curve, a small peak
22 at 1750 cm⁻¹, typical of C=O carbonyl group, is slightly visible. This peak indicates a non-
23 negligible presence of GTA in the sample 1:1. The large peaks detected at around 1070 e 1024 cm⁻¹
24 correspond to the CO bending vibration, typical of CH saccharidic structure.

25 Therefore, from FTIR analysis, two considerations can be made: 1) the cross-linking process
26 of CH with GTA has been successfully obtained, as demonstrated by the presence of the well

1 detectable peak at 1590 cm^{-1} in all the curves of cross-linked samples (imine C=N bond); 2) GTA
2 has been almost completely removed from the hydrogels, except for the 1:1 sample, in which the
3 carbonyl peak at 1750 cm^{-1} (belonging to free GTA) is non negligible. The latter result was,
4 however, expected, since in the 1:1 sample the excess of GTA was increased over a reasonably
5 necessary amount to set an upper limit to the use of GTA.



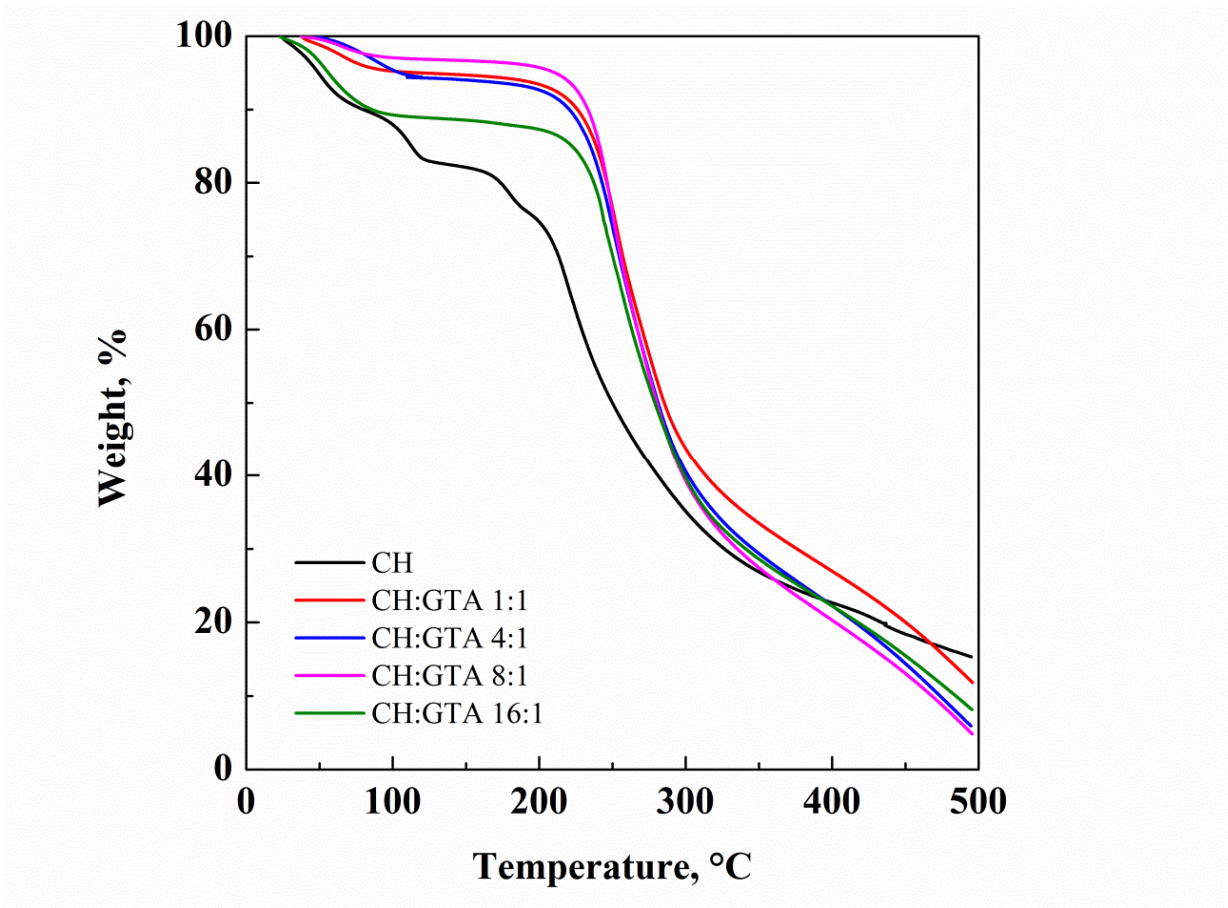
6 **Figure 4.** FTIR spectra of pure CH and CH aerogels, 2 % w/w crosslinked with GTA.

8 3.3 TGA analysis

10 In Figure 5 and in Table 3, thermogravimetric curves and decomposition temperatures (T_d)
11 of CH aerogels are reported. A comparison between the decomposition temperatures (T_d) shows
12 that CH aerogel has a T_d equal to $218\text{ }^\circ\text{C}$, whereas the crosslinked CH samples show higher T_d s,
13 which increase with the amount of crosslinking agent (from $247\text{ }^\circ\text{C}$ for CH:GTA 16:1 to $251\text{ }^\circ\text{C}$ for
14 CH:GTA 1:1). These data are consistent with the fact that the crosslinking reaction leads to a more

1 thermally stable structure, and to a consequent increased degradation temperature of the CH aerogel
 2 samples.

3



4

5 **Figure 5.** Thermogravimetric analysis of CH aerogel samples.

6

Aerogel	T_d^* , °C
CH	218
CH:GTA 16:1	247
CH:GTA 8:1	248
CH:GTA 4:1	249
CH:GTA 1:1	251

7 ^{*} T_d = Degradation temperature, corresponding to the maximum weight loss of the sample.

8 **Table 3.** Degradation temperature of CH aerogels crosslinked with GTA.

1 **4 Conclusions**

2 SC-CO₂ drying was successfully applied for the attainment of CH aerogels. GTA residues
3 measurements confirm that CH hydrogels crosslinked with GTA were successfully dried,
4 preserving their nanostructure: indeed, no collapse of the nanostructure was observed in the
5 aerogels surface and section. The hypothesis that SC-(CO₂ + ethanol) mixture is able to efficiently
6 extract GTA residues entrapped in the gel matrix was verified and negligible residues of GTA were
7 measured during release experiments.

8 Therefore, the produced CH aerogels not only maintained their delicate nanostructure
9 necessary for the cells cultivation, but can also be safely used for TE applications.

10

1 **References**

2

- 3 Adami, R., Liparoti, S., & Reverchon, E. (2011). A new supercritical assisted atomization configuration, for
4 the micronization of thermolabile compounds. *Chemical Engineering Journal*, *173*(1), 55-61.
- 5 Alves, N. M., & Mano, J. F. (2008). Chitosan derivatives obtained by chemical modifications for biomedical
6 and environmental applications. *International Journal of Biological Macromolecules*, *43*(5), 401-414.
- 7 Baldino, L., Cardea, S., De Marco, I., & Reverchon, E. (2014). Chitosan scaffolds formation by a supercritical
8 freeze extraction process. *The Journal of Supercritical Fluids*, *90*, 27-34.
- 9 Baldino, L., Cardea, S., & Reverchon, E. (2014). Supercritical assisted enzymatic membranes preparation, for
10 active packaging applications. *Journal of Membrane Science*, *453*(0), 409-418.
- 11 Barnes, C. P., Sell, S. A., Boland, E. D., Simpson, D. G., & Bowlin, G. L. (2007). Nanofiber technology:
12 Designing the next generation of tissue engineering scaffolds. *Advanced drug delivery reviews*, *59*(14),
13 1413-1433.
- 14 Barry, J., Gidda, H., Scotchford, C., & Howdle, S. (2004). Porous methacrylate scaffolds: supercritical fluid
15 fabrication and in vitro chondrocyte responses. *Biomaterials*, *25*(17), 3559-3568.
- 16 Berger, J., Reist, M., Mayer, J. M., Felt, O., Peppas, N. A., & Gurny, R. (2004). Structure and interactions in
17 covalently and ionically crosslinked chitosan hydrogels for biomedical applications. *European Journal of*
18 *Pharmaceutics and Biopharmaceutics*, *57*(1), 19-34.
- 19 Bigi, A., Cojazzi, G., Panzavolta, S., Rubini, K., & Roveri, N. (2001). Mechanical and thermal properties of
20 gelatin films at different degrees of glutaraldehyde crosslinking. *Biomaterials*, *22*(8), 763-768.
- 21 Cardea, S., Baldino, L., Pisanti, P., & Reverchon, E. (2014). 3-D PLLA scaffolds formation by a supercritical
22 freeze extraction assisted process. *Journal of Materials Science: Materials in Medicine*, *25*(2), 355-362.
- 23 Cardea, S., Baldino, L., Scognamiglio, M., & Reverchon, E. (2014). 3D PLLA/Ibuprofen composite scaffolds
24 obtained by a supercritical fluids assisted process. *Journal of Materials Science: Materials in Medicine*,
25 *25*(4), 989-998.
- 26 Cardea, S., & Reverchon, E. (2011). Nanostructured PVDF-HFP membranes loaded with catalyst obtained by
27 supercritical CO₂ assisted techniques. *Chemical Engineering and Processing: Process Intensification*, *50*(7),
28 630-636.
- 29 Choy, Y. B., Cheng, F., Choi, H., & Kim, K. K. (2008). Monodisperse gelatin microspheres as a drug delivery
30 vehicle: release profile and effect of crosslinking density. *Macromolecular bioscience*, *8*(8), 758-765.
- 31 Dash, M., Chiellini, F., Ottenbrite, R., & Chiellini, E. (2011). Chitosan—A versatile semi-synthetic polymer in
32 biomedical applications. *Progress in Polymer Science*, *36*(8), 981-1014.
- 33 De Marco, I., Knauer, O., Cice, F., Braeuer, A., & Reverchon, E. (2012). Interactions of phase equilibria, jet
34 fluid dynamics and mass transfer during supercritical antisolvent micronization: The influence of solvents.
35 *Chemical Engineering Journal*, *203*, 71-80.
- 36 Della Porta, G., Del Gaudio, P., De Cicco, F., Aquino, R. P., & Reverchon, E. (2013). Supercritical drying of
37 alginate beads for the development of aerogel biomaterials: optimization of process parameters and
38 exchange solvents. *Industrial & Engineering Chemistry Research*, *52*(34), 12003-12009.
- 39 Diamond, L. W., & Akinfiev, N. N. (2003). Solubility of CO₂ in water from -1.5 to 100 °C and from 0.1 to 100
40 MPa: evaluation of literature data and thermodynamic modelling. *Fluid Phase Equilibria*, *208*(1-2), 265-290.
- 41 Du, Z., Shen, Y.-B., Tang, C., Guan, Y.-X., Yao, S.-J., & Zhu, Z.-Q. (2014). Supercritical fluid assisted production
42 of chitosan oligomers micrometric powders. *Carbohydrate Polymers*, *102*, 400-408.
- 43 Duarte, A. R. C., Mano, J. F., & Reis, R. L. (2009). Preparation of starch-based scaffolds for tissue engineering
44 by supercritical immersion precipitation. *The Journal of Supercritical Fluids*, *49*(2), 279-285.
- 45 Dutta, P. K., Dutta, J., & Tripathi, V. (2004). Chitin and chitosan: Chemistry, properties and applications.
46 *Journal of Scientific and Industrial Research*, *63*(1), 20-31.
- 47 Eichhorn, S. J., & Sampson, W. W. (2005). Statistical geometry of pores and statistics of porous nanofibrous
48 assemblies. *Journal of The Royal Society Interface*, *2*(4), 309-318.
- 49 García-González, C., Alnaief, M., & Smirnova, I. (2011). Polysaccharide-based aerogels—Promising
50 biodegradable carriers for drug delivery systems. *Carbohydrate Polymers*, *86*(4), 1425-1438.

1 Harish Prashanth, K. V., & Tharanathan, R. N. (2007). Chitin/chitosan: modifications and their unlimited
2 application potential—an overview. *Trends in Food Science & Technology*, 18(3), 117-131.

3 Ho, M.-H., Kuo, P.-Y., Hsieh, H.-J., Hsien, T.-Y., Hou, L.-T., Lai, J.-Y., & Wang, D.-M. (2004). Preparation of
4 porous scaffolds by using freeze-extraction and freeze-gelation methods. *Biomaterials*, 25(1), 129-138.

5 Jin, R., Moreira Teixeira, L. S., Dijkstra, P. J., Karperien, M., Zhong, Z., & Feijen, J. (2008). Fast in-situ
6 formation of dextran-tyramine hydrogels for in vitro chondrocyte culturing. *Journal of Controlled Release*,
7 132(3), e24-e26.

8 Karimi, M., Heuchel, M., Weigel, T., Schossig, M., Hofmann, D., & Lendlein, A. (2012). Formation and size
9 distribution of pores in poly(ϵ -caprolactone) foams prepared by pressure quenching using supercritical CO₂.
10 *The Journal of Supercritical Fluids*, 61(0), 175-190.

11 Krajewska, B., Zaborska, W., & Leszko, M. (1997). Inhibition of chitosan-immobilized urease by boric acid as
12 determined by integration methods. *Journal of Molecular Catalysis B: Enzymatic*, 3(5), 231-238.

13 Kurita, K., Yoshino, H., Nishimura, S.-I., Ishii, S., Mori, T., & Nishiyama, Y. (1997). Mercapto-chitins: a new
14 type of supports for effective immobilization of acid phosphatase. *Carbohydrate Polymers*, 32(3-4), 171-
15 175.

16 Lee, K. Y., & Mooney, D. J. (2001). Hydrogels for tissue engineering. *Chemical reviews*, 101(7), 1869-1880.

17 Lee, Y.-G., Kang, H.-S., Kim, M.-S., & Son, T.-I. (2008). Thermally crosslinked anionic hydrogels composed of
18 poly(vinyl alcohol) and poly(γ -glutamic acid): Preparation, characterization, and drug permeation behavior.
19 *Journal of applied polymer science*, 109(6), 3768-3775.

20 Lin, W.-C., Yu, D.-G., & Yang, M.-C. (2006). Blood compatibility of novel poly (γ -glutamic acid)/polyvinyl
21 alcohol hydrogels. *Colloids and Surfaces B: Biointerfaces*, 47(1), 43-49.

22 Liparoti, S., Adami, R., & Reverchon, E. (2012). PEG micronization by supercritical assisted atomization,
23 operated under reduced pressure. *The Journal of Supercritical Fluids*, 72, 46-51.

24 Lv, Q., Hu, K., Feng, Q., & Cui, F. (2008). Fibroin/collagen hybrid hydrogels with crosslinking method:
25 preparation, properties, and cytocompatibility. *Journal of Biomedical Materials Research Part A*, 84(1), 198-
26 207.

27 Ma, L., Gao, C., Mao, Z., Zhou, J., Shen, J., Hu, X., & Han, C. (2003). Collagen/chitosan porous scaffolds with
28 improved biostability for skin tissue engineering. *Biomaterials*, 24(26), 4833-4841.

29 Ma, P. X. (2004). Scaffolds for tissue fabrication. *Materials today*, 7(5), 30-40.

30 Marra, F., De Marco, I., & Reverchon, E. (2012). Numerical analysis of the characteristic times controlling
31 supercritical antisolvent micronization. *Chemical Engineering Science*, 71, 39-45.

32 Montes, A., Gordillo, M. D., Pereyra, C., De los Santos, D. M., & Martínez de la Ossa, E. J. (2014). Ibuprofen-
33 polymer precipitation using supercritical CO₂ at low temperature. *The Journal of Supercritical Fluids*, 94(0),
34 91-101.

35 Park, H., Park, K., & Shalaby, W. S. (2011). *Biodegradable hydrogels for drug delivery*. CRC Press.

36 Park, J., & Lakes, R. S. (2007). *Biomaterials: an introduction*. Springer.

37 Payne, G. F., Chaubal, M. V., & Barbari, T. A. (1996). Enzyme-catalysed polymer modification: Reaction of
38 phenolic compounds with chitosan films. *Polymer*, 37(20), 4643-4648.

39 Pisanti, P., Yeatts, A. B., Cardea, S., Fisher, J. P., & Reverchon, E. (2012). Tubular perfusion system culture of
40 human mesenchymal stem cells on poly-L-lactic acid scaffolds produced using a supercritical carbon
41 dioxide-assisted process. *Journal of Biomedical Materials Research Part A*, 100(10), 2563-2572.

42 Quirk, R. A., France, R. M., Shakesheff, K. M., & Howdle, S. M. (2004). Supercritical fluid technologies and
43 tissue engineering scaffolds. *Current Opinion in Solid State and Materials Science*, 8(3-4), 313-321.

44 Ravi Kumar, M. N. V. (2000). A review of chitin and chitosan applications. *Reactive and Functional Polymers*,
45 46(1), 1-27.

46 Reverchon, E., & Cardea, S. (2012). Supercritical fluids in 3-D tissue engineering. *The Journal of Supercritical
47 Fluids*, 69, 97-107.

48 Reverchon, E., Cardea, S., & Rapuano, C. (2008). A new supercritical fluid-based process to produce
49 scaffolds for tissue replacement. *The Journal of Supercritical Fluids*, 45(3), 365-373.

50 Sabirzyanov, A. N., Il'in, A. P., Akhunov, A. R., & Gumerov, F. M. (2002). Solubility of Water in Supercritical
51 Carbon Dioxide. *High Temperature*, 40(2), 203-206.

- 1 Speer, D. P., Chvapil, M., Eskelson, C., & Ulreich, J. (1980). Biological effects of residual glutaraldehyde in
2 glutaraldehyde-tanned collagen biomaterials. *Journal of biomedical materials research*, 14(6), 753-764.
- 3 Yang, S., Leong, K.-F., Du, Z., & Chua, C.-K. (2001). The design of scaffolds for use in tissue engineering. Part
4 I. Traditional factors. *Tissue engineering*, 7(6), 679-689.
- 5 Zeiger, E., Gollapudi, B., & Spencer, P. (2005). Genetic toxicity and carcinogenicity studies of
6 glutaraldehyde—a review. *Mutation Research/Reviews in Mutation Research*, 589(2), 136-151.

7

8